Characterization and Application of Nanomaterials 2026, 9(1), 8340.
https://doi.org/10.24294/can8340

Article

Green synthesis of silver nanoparticles using *Camellia sinensis* (tea) leaves extract: Characterization and study of its antimicrobial activities

Nuna Magar, Pujan Nepal, Asmita Thapa Magar, Jamuna Thapa Magar, Hari Bhakta Oli*, Deval Prasad Bhattarai*

Department of Chemistry, Amrit Campus, Tribhuvan University, Kathmandu 44600, Nepal
*** Corresponding authors:** Hari Bhakta Oli, hari.oli@ac.tu.edu.np; Deval Prasad Bhattarai, deval.bhattarai@ac.tu.edu.np

CITATION

Magar N, Nepal P, Magar AT, et al. Green Synthesis of Silver Nanoparticles Using *Camellia sinensis* (Tea) Leaves Extract: Characterization and Study of Its Antimicrobial Activities. Characterization and Application of Nanomaterials. 2026; 9(1): 8340. https://doi.org/10.24294/can8340

ARTICLE INFO

Received: 1 August 2024
Accepted: 24 February 2026
Available online: 20 March 2026
2026

Abstract: Chemical synthesis of nanoparticles is costly, harmful to the environment, and less efficient in terms of materials and energy demand. Therefore, the synthesis of ecologically friendly nanoparticles that do not produce harmful waste throughout the manufacturing process has piqued the curiosity of researchers. This can be accomplished by using biological synthesis procedures that are regarded as safe and environmentally friendly compared to traditional physical and chemical methods. Herein, tea (*Camellia sinensis*) leaf extract was used to synthesize the silver nanoparticles (AgNPs). Ultra-violet-visible spectrophotometry (UV-Vis), X-ray diffraction (XRD), Zeta potential, Fourier Transform Infrared (FTIR) spectroscopy, Field Emission Scanning Electron Microscopy (FESEM), and Energy Dispersive Spectroscopy (EDX) were used to characterize the as-synthesized AgNPs. The surface plasmon resonance (SPR) peak of AgNPs was observed at 400–500 nm in UV-Vis spectra. The band gap energy of 3.605 eV was computed by Tauc's plot analysis, suggesting the semiconductor applications of AgNPs. The size of AgNPs estimated from FESEM was 66.87 ± 16.74 nm. EDX analysis confirmed the AgNPs' purity with a strong silver signal at 3 keV. The evaluation of antimicrobial activity of AgNPs against Gram-negative bacterium (*Escherichia coli*), Gram-positive bacterium (*Bacillus subtilis*), and pathogenic fungus (*Candida albicans*) was carried out. The zone of inhibition (ZOI) exhibited against those microbes was respectively 12, 11, and 10 mm, against the 20 mm ZOI exhibited by the control kanamycin. These corroborating facts have led to the conclusion that *Camellia sinensis* leaf extract is suitable for the environmentally friendly synthesis of AgNPs with potential antimicrobial uses.

Keywords: *Camellia sinensis;* leaf extract; silver nanoparticles; green synthesis; tauc's plot; antimicrobial actives

1. Introduction

Nanoparticle synthesis through conventional chemical and physical methods often requires expensive equipment, high energy input, and complex processing steps. Furthermore, the majority of chemicals used in these synthetic routes are hazardous, toxic, and their improper handling or disposal can pose serious risks to human health and the environment. The incorporated toxic residual chemicals during the synthesis and processing of nanoparticles can limit their suitability for biomedical and clinical applications [1]. Consequently, there is a growing interest in green synthesis methods for nanoparticle synthesis, which eliminates or minimizes the use of hazardous chemicals and prevents the formation of toxic byproducts. In this respect, the demand for "green nanotechnology" seems to be growing [2].

The nanoparticles of noble metals such as Palladium, Tin, Copper [3], Silver [2,4], and Gold [5] are now receiving considerable interest due to their unique characteristics

and applications in various sectors. Among them, AgNPs are one of the most important and intriguing nanoparticles having significant biomedical applications. AgNPs can be synthesized by the chemical reduction method, such as the reduction of silver ions from silver nitrate precursor using hydrazine hydrate as a reducing agent [6]. But hydrazine hydrate is a hazardous chemical. The biological approach involves nanoparticle synthesis using bacteria, fungi, and plant extracts. Plant extracts have often been employed as reducing agents instead of chemical reducing agents in this technique. Therefore, there is no need to introduce any hazardous substances, as the process is renewable and affordable [7].

Silver nanoparticles (AgNPs) find diverse applications in molecular diagnostics, therapeutic interventions, antimicrobial applications, and various medical devices due to their high surface-to-volume ratio and unique physicochemical properties [8]. Besides, AgNPs find their applications in electronics, biosensors, catalysis, photonics, and optoelectronics due to their good electrical conductivity and chemical stability [9]. Since ancient times, metallic silver as well as other silver compounds have been well-recognized for their antimicrobial properties and have been used in burns, wounds, and antibacterial infections [10]. Nevertheless, those applications opened the windows, but their efficiencies were measurable. So in the modern society, AgNPs has been reported to use to induce apoptosis (a programmed cell death) more strongly than necrosis in cancer cell lines [11], which has also been reported against different cell lines: gastric cancer cells [12], human breast cancer cell (MCF-7), and human colon carcinoma cell (HCT-116) [13]. AgNPs show antimicrobial, antifungal [14], antioxidant [15], anti-diabetic [16], and anti-inflammatory effects, making them promising candidates for the development of novel and cost-effective pharmaceutical drugs [17]. The AgNPs synthesized using the green approach can exhibit good activity against isolated dermatophytes, which can be utilized to develop drug-resistant, broad-spectrum antibiotics and aid in treating various types of wounds and burns [18]. Additionally, they possess the ability to act in oral rehydration solutions and disinfectants. AgNPs have been shown to improve and prolong the performance of drugs and targeted drug delivery systems [18]. In addition, silver nanoparticles are essential in the pharmaceutical industry because they serve as antibacterial agents with minimal toxic effects [19].

Antibiotic resistance is one of the world's greatest health risks, and microbial resistance grows faster than the current rate of discovering new and effective medicines. To counter these antibiotic-resistant microorganisms, metal-based antimicrobial substances such as AgNPs with readily adjusted physicochemical characteristics can be prepared. AgNPs have a broad antibacterial impact as they can damage the extracellular membrane and intracellular components of bacteria. The AgNPs used as antimicrobial agents in the medicinal field release silver ions, and those ions primarily exhibit antibacterial and antifungal properties [20].

Green synthesis is the creation of nanoparticles using environmentally friendly components obtained from bacteria, fungi, and plants, and they are free of the drawbacks that come with traditional synthetic techniques [21]. It has been reported that extracts obtained from yeast, bacteria, actinomycetes, fungi, algae, and plants can be used to synthesize AgNPs [22]. The secondary metabolites, like alkaloids, flavonoids, terpenoids, steroids, amino acids, phenolics, saponins, polysaccharides,

etc., present in plant extract, are responsible for the reduction of metal ions to metallic nanoparticles [23] and serving as a capping agent. Despite numerous studies reporting on AgNPs synthesis by the green synthesis route, there are still some lacunae in the identification of suitable phytochemicals. A core challenge is compounded by the difficulties in scaling up synthesis due to variable plant cultivation conditions, diverse chemical profiles, and flexible extraction parameters. For this, extensive research must be done in this area.

Previous experiments have explored the possibility of synthesizing AgNPs using *Camellia sinensis* extract, demonstrating some good antimicrobial activities [24], photocatalytic activities [25], antioxidant and anti-inflammatory properties [26]. Some of the researchers have also studied the effect of pH, temperature, and time on the extraction of phytochemicals from *Camellia sinensis* [27]. Nevertheless, experiments have been done, but the origin of phytochemicals strongly varies based on the climate, altitude, and soil texture. The phytochemicals have the principal role in the synthesis of AgNPs. So, this study explores the green synthesis of AgNPs using the aqueous extract of *Camellia sinensis* leaves of Nepali origin. *Camellia sinensis,* a plant native to Southeast Asia of the *Camellia* genus, is now at the forefront of being used in the synthesis of nanoparticles [28]. *Camellia sinensis* is a perennial shrub that helps to stabilize steep mountain slopes, mitigating erosion and fostering microhabitats for flora and fauna in anthropogenic landscapes of Ilam, Nepal. Culturally, it sustains traditional agrarian practices and serves as the centerpiece of communal rituals (masala tea blends). Indigenous groups have long harnessed the polyphenol-rich leaves to soothe digestive discomfort and reduce inflammation, aligning with broader Himalayan ethnomedicinal traditions. *Camellia sinensis* leaves contain polyphenolic chemicals that include epigallocatechin, caffeine, tannins, catechin, and epicatechin, which protect plants from dangerous infections in addition to free-radical scavenging and antioxidant activities. Such types of phytochemicals can be used as simultaneous reductants as well as capping agents for AgNPs synthesis.

This research aims to develop an eco-friendly, cost-effective synthesis strategy for AgNPs using *Camellia sinensis* leaf extract as both a reducing and stabilizing agent, as a sustainable alternative to conventional AgNPs synthesis approaches that rely on hazardous chemicals and incur high production costs. The study further seeks to systematically characterize the physicochemical properties of the leaf extract-mediated AgNPs and evaluate their antimicrobial efficacy against a panel of Gram-positive, Gram-negative bacteria, and pathogenic fungi. Collectively, these investigations are designed to assess the potential of biosynthesized AgNPs for dual applications in semiconductor and antimicrobial fields, thereby expanding the practical utility of green-synthesized nanomaterials for industrial and biomedical use.

2. Experimental section

2.1. Sample collection and experimental site

Tea (*Camellia sinensis*) leaves were collected from Ilam, Nepal, in March 2022. The scientific name of the plant was ensured by the Department of Botany, Amrit Campus, Tribhuvan University, Kathmandu, Nepal, by the herbarium matching

method. The synthesis of AgNPs was carried out in the Chemistry Research Laboratory of Amrit Campus.

2.2. Preparation of *Camellia sinensis* extract

Tea (*Camellia sinensis*) leaves were cleaned and dried in the shade to eliminate any remaining water on their surface. Then, 10 g of finely cut dry tea leaves were heated at 60 ℃ for 15 min in 100 mL of distilled water in a beaker. Whatman filter No.1 paper (cellulose filters, 90 mm diameter, pore size 11 μm) was used to filter the supernatant solution. The light-brown transparent solution was obtained, which was labeled as an aqueous extract and then kept at 4–8 ℃ in freeze.

2.3. Green synthesis of AgNPs

In a conical flask, 10 mL of freshly prepared extract was taken, and 100 mL of 0.1 M $AgNO_3$ was added dropwise from the burette to the extract on a continuous stirring mode in the magnetic stirrer. The drop rate was so adjusted that the addition of the whole solution to the flask took 30 min. The solution mixture was stirred constantly on a magnetic stirrer for an hour at room temperature. During the time of stirring, a reddish-brown-colored suspension was obtained. The formation of AgNPs was noticed as a color change in the solution appeared. After the formation of the suspension, it was centrifuged for 10 min at 12,500 rpm, and the supernatant liquid was discarded, whereas the residue was washed with distilled water followed by ethanol. Centrifugation and decantation, followed by a washing process, were repeated to remove possible impurities. The obtained mass was dried to obtain the AgNPs in solid form.

2.4. Physicochemical characterization

The formation of AgNPs was monitored by observing the color change of the solution as well as by recording absorbance spectra using a double-beam UV-vis spectrophotometer (Labtronics, LT-2802) in the wavelength range of 300–700 nm at a scan interval of 5 nm. Fourier Transform Infra-red (PerkinElmer 10.6.2) spectrometer in attenuated total reflectance (ATR) mode was used to study the functional group of phytochemicals in the range of 500–4000 cm^{-1}. The zeta potential measurements of the AgNPs were carried out using a Nanopartica nanoparticle analyzer (SZ-100V2, Horiba Scientific) at Nepal Academy of Science and Technology (NAST), Nepal. Zeta potential measurements were conducted at 25 ℃ using an aqueous dispersion of the particle at pH 6.78. An X-ray diffractometer (Rigaku, Japan, CuKa = 1.5406 Å) was used to collect the diffraction pattern of AgNPs within 10–80 ° diffraction angle and scan of 5 °/min at 0.02 ° steps. Likewise, the surface morphology and elemental analysis were carried out using FESEM (Hitachi, Tokyo, Japan) equipped with energy dispersive X-ray spectroscopy (EDX), and transmission electron microscopic measurement (HR-TEM, JEM-2200, JEOL, Japan). Antibacterial and antifungal tests were carried out at the Himalayan Research Institute, Nepal.

2.5. Antibacterial test of the synthesized AgNPs

Clinical isolates of *Escherichia coli*, *Bacillus subtilis*, and *Candida albicans* were tested. Mueller Hinton agar medium was used to incubate the single colony of each test strain in a temperature-controlled shaker at 37 ℃ overnight. An autoclaved petri dish and agar medium where microbial culture has been made were used to determine the zone of inhibition (ZOI) by the disc diffusion method. Three separate plates for each microbe in agar media were taken, and two discs in each plate were fixed at equal distances. The 50 μg of AgNPs as powder in the first disk and 50 μg of reference antibiotic kanamycin in the second disk were loaded. These plates were then incubated overnight at 37 ℃. After incubation, the ZOI was measured and compared. Water was used as a negative control, and triplicate measurements were carried out to ensure reproducibility.

3. Results and discussion

3.1. Visual observation

The appearance of a reddish-brown color in the solution mixture of precursor and aqueous extract observed indicates the bio-reduction of silver ions to silver nanoparticles. The progressive change in color of different mixtures from the beginning is shown in **Figure 1a–d**. The color change was observed with the increase in stirring time. The color change further indicated that the plant started to reduce the silver nitrate solution. Hence, the tea extract was effective in reducing the silver nitrate solution, and silver nanoparticles were obtained. Studies also reported that the phytoconstituents in tea leaves extract, like phenolics, flavonoids, terpenoids, polysaccharides, etc., can reduce Ag^{+} to Ag^{0} [28,29].

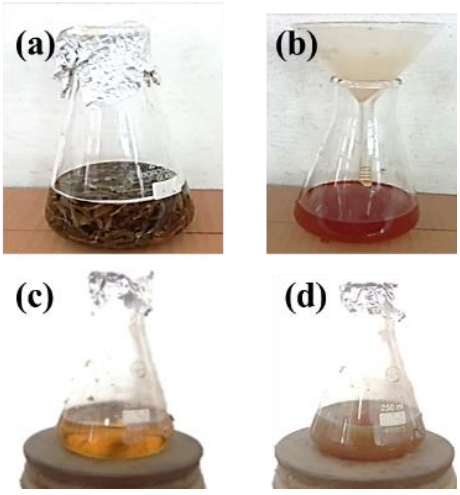

Figure 1. Visual observation of silver nanoparticle formation: (**a**) tea leaves boiled in distilled water, (**b**) aqueous extract, (**c**) mixture of an aqueous extract with the precursor, (**d**) after formation of AgNPs.

3.2. UV-visible spectra and Tauc plot

The absorption spectra of colloidal dispersion of AgNPs in ethanol (**Figure 2a**) show the absorption peak maxima at 425 nm, which is the characteristic peak of

AgNPs and is associated with its surface plasmon resonance (SPR) absorbance. The broad spectrum of AgNPs synthesized using *Camellia sinesis* extract at 436 nm is also reported by Loo et al. [30]. The broad peak at 425 nm with a large half-width of the AgNPs and hump around 450 nm may be either large-sized or agglomerated AgNPs [25].

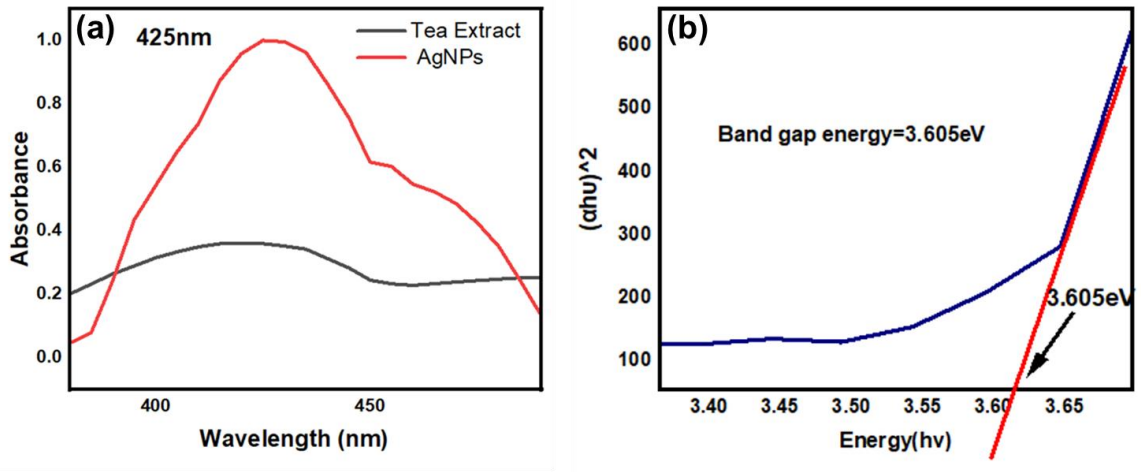

Figure 2. UV-VIS spectra and band gap study: (**a**) UV-visible spectra of AgNPs and (**b**) band gap calculated from the Tauc plot.

Monitoring of the formation of AgNPs was carried out by recording absorbance spectra at regular time intervals in the range of 200–600 nm, where the increase in the absorbance intensity at 425 nm indicated the formation of AgNPs. Similar results, including a color transition from a light yellow to brown color and a well-defined absorption peak at 438 nm for the use of *O. basilicum*, and 439 nm for the use of *Camellia sinensis*, have been reported in the literatures [31,32]. In a similar work, the synthesized AgNPs exhibited an absorption peak at 416 nm using *Annona reticulata* [33]; 430 nm using *Origanum vulgare* [34]; 435 nm using *Givotia moluccana* leaf extract [35]; 430 nm using *Artemisia vulgaris* leaf extract [36]. The optical band gap of as-synthesized AgNPs was determined by extrapolation of the linear portion of the Tauc plot of $(\alpha h\nu)^2$ over a limited range of photon energies hν, as shown in **Figure 2b**. The band gap was found to be 3.605 eV, indicating that the AgNPs exhibit a quantum confinement effect. The higher band gap energy indicates not only antimicrobial activity of the AgNPs but also suggests their potential applicability in optoelectronic devices. A similar band gap energy value was also reported in the literature elsewhere [37].

3.3. FTIR studies

FTIR spectra of AgNPs obtained by the green synthesis method with the extract of *Camellia sinensis* have been recorded and presented in **Figure 3**. The peak at 3267 cm^{-1} is attributed to -OH vibrational stretching of polyphenols (catechins and tannins) [4,38,39]. The strong absorbance peak at 1621 cm^{-1} is attributed to the C=O/C=C stretching, particularly the carbonyl group or amide I band or conjugated carbon [40]. A band observed at ~1191 cm^{-1} corresponds to the C-O stretching of alcohol, phenol,

or ester group present in phytochemicals [38]. From the FTIR analysis, the bands observed at 597, 667, 1191, 1339, 1501, 1621, and 3267 cm^{-1} in the pure extract are also observed in the AgNPs, with reduced intensity indicating the presence of capping and stabilizing biomolecules adsorbed on the surface of AgNPs. Additionally, these findings indicate that the hydroxyl (–OH) and carbonyl (C=O) functional groups play a significant role in the green synthesis of silver nanoparticles. Hydroxyl groups basically contribute to the reduction of silver ions to silver, while carbonyl groups are mainly involved in the stabilization and capping of the synthesized silver nanoparticles. Similar features were detected in previous reports on AgNPs synthesis observed by FTIR, indicating the contribution of capping agents as functional groups involved in the stabilization of AgNPs [32,33].

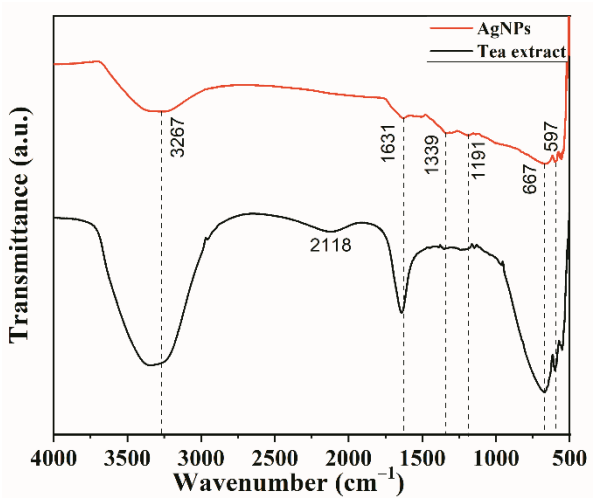

Figure 3. FTIR spectra of the extract and AgNPs.

3.4. Stability of AgNPs

The zeta potential of the silver nanoparticles (AgNPs) was measured to determine their surface charge and colloidal stability, and is shown in **Figure 4**. The AgNPs exhibited a zeta potential value of –43.04 mV, with a narrow single peak. The negative value indicates the negative surface charge of the silver nanoparticles. As the magnitude value of zeta potential is well above ±30 mV threshold, strong electrostatic repulsion exists among the AgNPs, effectively preventing their aggregation. According to the Derjaguin-Landau-Verwey-Overbeek (DLVO) theory, the high negative zeta potential value indicates that the electrostatic repulsive forces dominate over the weak van der Waals' attractive force, resulting in a stable nanoparticle dispersion [41]. Furthermore, the narrow peak suggests a relatively homogeneous particle population with a uniform surface charge, implying effective and consistent surface functionalization or capping. The strong negative charge is likely attributed to plant-derived polyphenols and deprotonated surface functional groups like $-COO^-$ and $-OH^-$, etc.

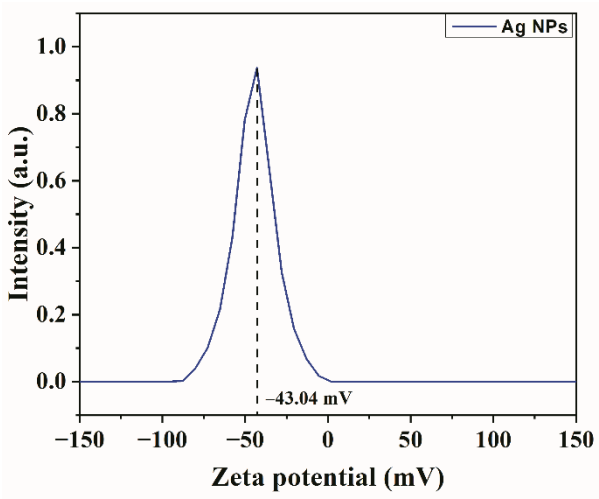

Figure 4. Zeta potential of Ag NPs prepared using *C. sinensis* extract.

3.5. X-ray diffraction (XRD) spectroscopic studies

The crystallographic orientation of the AgNPs was determined by recording an X-ray diffraction pattern, as shown in **Figure 5**. Diffraction angles corresponding to 2θ = 38.1°, 44.3°, 64.5°, and 77.3° were reflection planes (111), (200), (220), and (311), respectively (JCPDS No 87-0720) of the face-centered cubic (FCC) crystal of AgNPs. The results of these crystal planes proved that AgNPs were formed as a result of the reduction of Ag^+ ions from the precursor solution. The highly intense peak at 38.1 °corresponds to the (111) plane of the FCC of AgNPs [42]. The sharp and intense peaks of different crystal planes of the AgNPs showed that the synthesized NPs were highly crystalline and of high purity. The Debye-Scherrer equation was used to calculate the average grain size of the AgNPs using full width at half maximum (FWHM). The crystallite size estimated from the most intense peak was found to be 20.62 nm and varied up to 11.74 nm for different peaks, as given in **Table 1**. A similar crystallite size was reported by Singh et al. [43]. Similar diffraction peaks of the FCC crystal of AgNPs using *Annona reticulata* extract were reported at 37.56, 43.25, and 64.10 °, corresponding to (111), (200), and (220), respectively. Similar findings were also reported by other researchers [34,44].

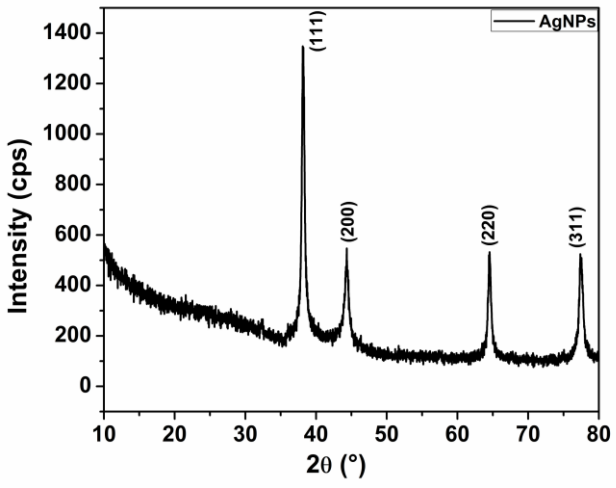

Figure 5. XRD pattern of AgNPs.

Table 1. d-spacing value, crystallite planes, FWHM, and crystallite size (D) of the synthesized AgNPs.

Plane	2θ (in degree)	θ (in degree)	d_{hkl} = nλ/2 sin θ in Å n = 1 and λ = 1.54Å	β (FWHM, in degree)	D = 0.9λ/βcosθ (in nm)
111	38.1	19.05	2.36	0.4258	20.62
200	44.3	22.15	2.04	0.7632	11.74
220	64.5	32.25	1.44	0.5876	16.70
311	77.3	38.65	1.23	0.6456	16.47

3.6. Surface morphology and elemental study

Surface morphological evidence of AgNPs was recorded using FESEM, and elemental mapping was carried out using EDX. The FESEM images of AgNPs captured at different magnifications are given in **Figure 6a–d**. The images show that the AgNPs are homogeneously formed with a narrow size distribution. This is evidenced by the measurement of the size of silver nanoparticles using ImageJ software. The result shows the particle size of 66.86 ± 16.73 nm. The silver nanoparticles are formed in nanorange. The particle sizes calculated via the Debye-Scherrer formula and SEM image analysis are 20.62 nm and 66.87 ± 16.74 nm, respectively. This significant difference is because the Debye-Scherrer formula only gives the crystallite size, but not the particle size of amorphous particles and agglomerated particles. However, the SEM image analysis gives the morphological size of the amorphous as well as agglomerated particles, but not crystallite size. The synthesized AgNPs get agglomerated so quickly, even in the presence of inhibitor molecules. This leads to a difference in the size of AgNPs, which is determined via XRD and SEM.

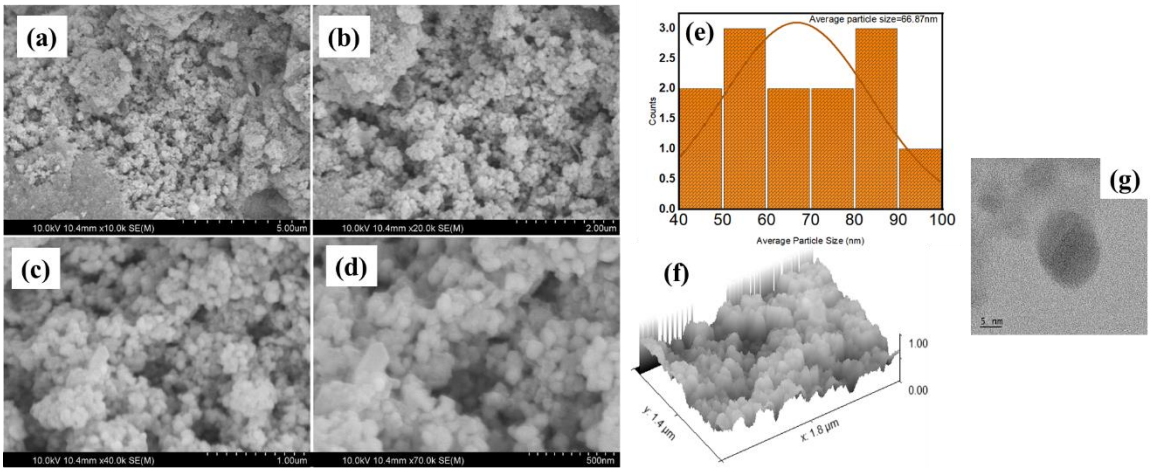

Figure 6. Field Emission Scanning Electron Microscopy (FESEM) of AgNPs at Different Magnification; (**a**) (×10,000) in 5 µm scale bar, (**b**) (×20,000) in 2 µm scale bar, (**c**) (×400,000) in 1 µm scale bar, (**d**) (×70,000) in 500 nm scale bar, (**e**) size histogram of AgNPs counted from SEM image, (**f**) 3D mapping of AgNPs, and (**g**) TEM image of synthesized AgNPs.

The study was found to be consistent with the literature [45]. **Figure 6e** shows the size histogram of AgNPs counted from the SEM image. **Figure 6f** shows the 3D image of the AgNPs in 500 nm (×70,000), and the frequency of FESEM size distribution of AgNPs was determined in this scale, with the particle size ranging from

28–74.42 nm. The average diameter of the synthesized AgNPs was calculated by measuring the particles in random fields of FESEM. Similarly, the TEM image of the AgNPs was recorded to confirm the size of the nanoparticle, and it is found in the nano range, as in **Figure 6g**. These results are in agreement with the findings of the FESEM image and grain size calculated using the Debye-Scherrer equation. Similar results were reported in other literature [46].

Elemental mapping of the AgNPs was performed using FESEM equipped with EDX, which is shown in **Figure 7**. The result predominantly shows a silver nanoparticle with some oxygen and carbon. As the XRD report supports the formation of silver nanoparticles but not silver oxide nanoparticles, the presence of carbon and oxygen is due to the presence of organic moieties from the aqueous extract of *Camellia sinensis.* The most intense and sharp peak at 3.0 keV in the EDX spectra indicates the presence of metallic Ag. Likewise, other peaks around 0.3 and 0.5 keV are those of C and O, respectively, which are obtained from the tea leaves extract. From the study, the optical absorption peak at 3 keV indicated the presence of silver nanoparticles with excellent purity, as reported in the literature [45,46].

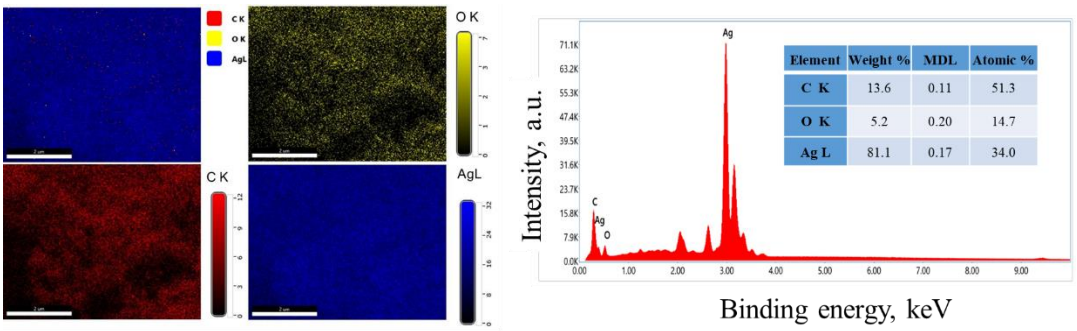

Figure 7. Elemental Maps based on Energy-Dispersive X-ray measurements.

3.7. Antimicrobial study

The antimicrobial activity exhibited by the synthesized AgNPs was comparable to that of the standard antibiotic. The ZOI calculation for the Gram-negative bacterial samples of *E. coli* (aqueous cultures), Gram-positive bacterial samples of *B. subtilis*, and the fungus of *Candida albicans* was determined by treating with concentrations of 50 µg of AgNPs for 24 h.

From the experimental evidence in **Table 2**, the ZOI shown by AgNPs for *E. coli* was 12 ± 0.009 mm, for *B. subtilis* was 11 ± 0.02 mm, and for the fungus was 10 ± 0.01 mm, indicating that the synthesized AgNPs are more effective for Gram-negative bacteria in comparison to others. It can be concluded that AgNPs obtained using tea extract have good antibacterial potential [31]. The ZOI shown by the AgNPs against three different microbes is shown in **Figure 8**. Similar results were observed where bacterial strains of *E. coli*, *S. aureus*, and *P. aeruginosa* also indicated the distinct antimicrobial potential of AgNPs. In some literatures, the effectiveness of AgNPs for *E.coli* was found to be higher than *S. aureus*, where AgNPs were synthesized using *Berberis vulgaris* leaf and root extract [31], whereas leaf extract of neem and tea-mediated AgNPs were more effective against Gram-positive bacteria than against Gram-negative ones.

Table 2. Zone of Inhibition shown by AgNPs for selected bacteria observed after 24 h exposure test (Mean ± SD, n = 3).

Microorganisms test organism (ATCC)	**Reference culture**	**Type**	**Zone of inhibition (ZOI) (mm)**	
			AgNPs	(+ve Control)
Bacillus subtilis	ATCC 6633	Gram-positive Bacteria	11 ±0.02	20 ±0.003
Escherichia coli	ATCC 25922	Gram-negative Bacteria	12 ±0.009	20 ±0.002
Candida albicans	ATCC 10231	Gram-positive fungus	10 ±0.01	18 ±0.004

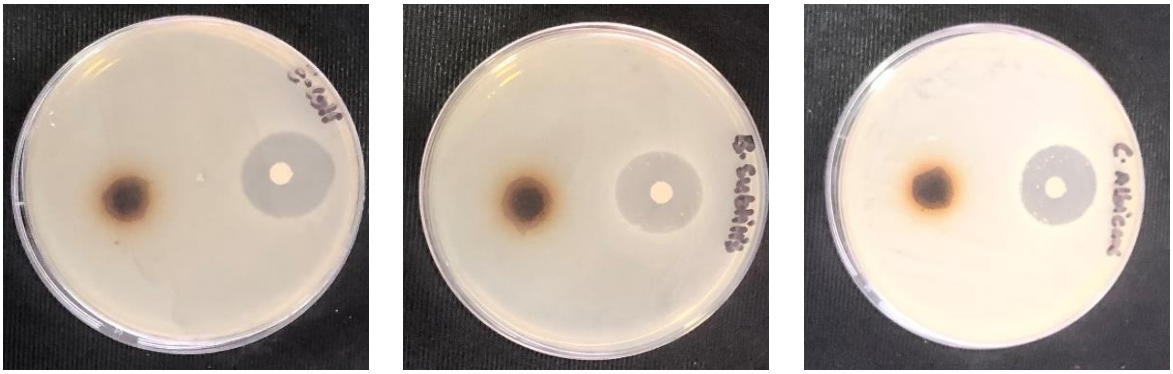

Figure 8. Zone of Inhibition Observed when Bacterial Strains are treated with AgNPs.

The antimicrobial activity of *Camellia sinensis* leaf extract-mediated AgNPs against *E. coli*, *B. subtilis*, and *C. albicans* demonstrates efficacy relative to state-of-the-art biosynthesized AgNPs, with the added advantage of a sustainable, low-cost synthesis route free of toxic reagents. A direct comparison with prior literature reveals notable consistency and competitiveness, as shown in **Table 3**.

Table 3. Antimicrobial activity of the synthesized AgNPs with some recent literature.

Source of extract	**Size of AgNPs (nm)**	**Microbial strains**	**ZOI (mm)**	**Reference**
Indigofera barberi leaf	5–20	*B. subtilis* *E. coli*	11.2 9.8	[47]
Mentha piperita leaf	20–70	*E. coli*	12.6 ±0.78	[48]
Ocimum sanctum leaf	4–98	*E. coli*	17	[49]
Adina cordifolia leaf	10–45	*B. subtilis* *E. coli*	12 ±3 13 ±3	[50]
Punica granatum peel	10–30	*B. subtilis*	11–6	[51]
Callistemon citrinus flower	20–70	*C. albicans*	9.5–17	[51]
Alchemilla vulgaris leaf *Melissa officinalis* leaf *Foeniculum vulgare* seed		*E. coli* *B. subtilis* *C. alibcans*	0, 0, 10 12, 22, 16 0, 10, 10	[52]
Rosmarinus officinalis leaf	10-33	*E. coli* *C. albicans*	7–9 11–17	[53]
Camellia sinensis leaf	66.87 ±16.74	*E. coli* *B. subtilis* *C. alibcans*	12 ±0.009 11 ±0.02 10 ±0.01	This study

3.8. Mechanism of antimicrobial activity of AgNPs

The antimicrobial efficacy of *C. sinensis*-mediated AgNPs is driven by a synergistic mechanism, which is facilitated by their physicochemical properties and surface-functionalized bioactive molecules. Synthesized AgNPs exhibit robust, broad-spectrum antimicrobial activity through a combination of membrane disruption, ion-mediated intracellular toxicity, and synergistic interactions with plant-derived functional groups, offering a sustainable alternative to conventional antimicrobial agents for biomedical and environmental applications, as shown in **Figure 9**.

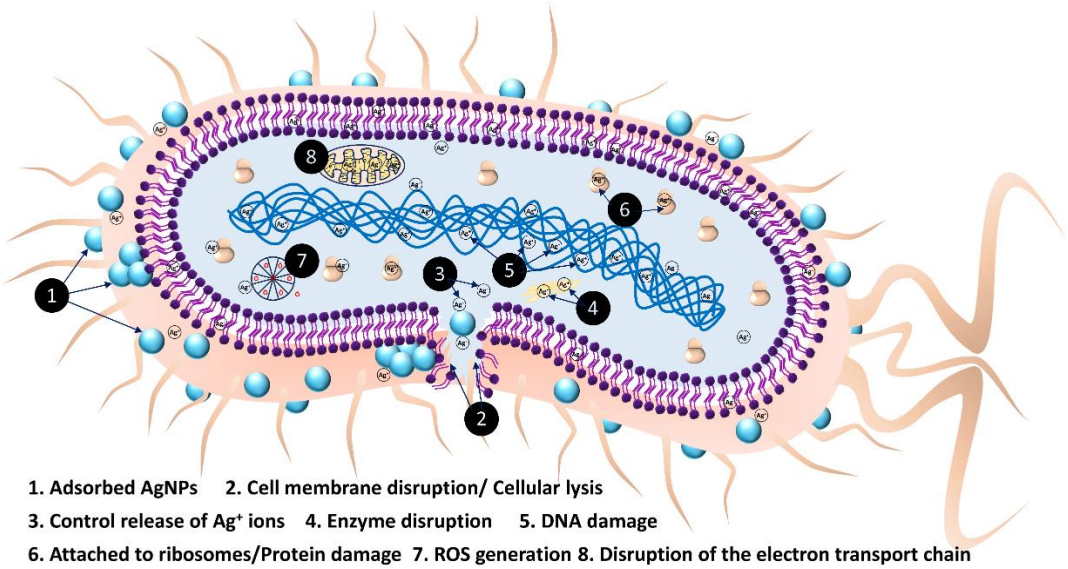

Figure 9. Schematic representation of the mechanism of antimicrobial activity of AgNPs.

The synthesized AgNPs get adsorbed on the membranes of bacteria and fungi, which either disrupt the cell membrane and lead to cell lysis [41,54–56] or the AgNPs gradually release Ag^+ ions into the microbial environment. These ions penetrate the cell cytoplasm and interfere with key metabolic pathways: they bind to thiol groups (-SH) of essential enzymes, inhibiting their catalytic activity [57], they interact with DNA, inducing double-strand breaks and preventing replication/transcription [58]; and they disrupt the mitochondrial electron transport chains, leading to the overproduction of reactive oxygen species (ROS) (e.g., O_2^-, H_2O_2) [54]. The accumulation of ROS further exacerbates lipid peroxidation, protein denaturation, and cellular damage [59]. Meanwhile, the polyphenolic compounds adsorbed on the AgNPs surfaces enhance antimicrobial activity independently and synergistically. They chelate essential microbial metal ions (e.g., Fe^{2+}, Zn^{2+}) necessary for microbial growth [53] and inhibit microbial enzyme activity [41]. This synergism enhances the overall antimicrobial efficacy, distinguishing biosynthesized AgNPs from chemically synthesized counterparts, which lack such natural adjuvants. The schematic diagram for the mechanism of antimicrobial activity of AgNPs is shown in **Figure 9**.

4. Conclusions

Camellia sinensis leaf extract effectively mediates the reduction of silver ions to metallic silver and exerts a stabilizing effect on the formed nanoparticles in their nanosizes. The UV-Vis spectral analysis of the synthesized AgNPs revealed a strong absorption band at 425 nm, which indicates the formation of AgNPs. The Tauc plot yielded an optical band gap of 3.605 eV, showing the potential application of these AgNPs as semiconductor materials. The XRD patterns exhibited an intense diffraction peak corresponding to the lattice plane of metallic silver, which verified the crystalline nature of the AgNPs with an average crystallite size of 20.62 nm (111). In contrast, the average particle size was 66.87 ± 16.74 nm from FESEM micrographs. EDX Analysis showed a sharp and intense peak of 3.0 keV, confirming the metallic silver. The antimicrobial activity assay of AgNPs exerted a concentration-dependent inhibitory effect on the tested microbes: the maximum ZOI was 12 mm for *Escherichia coli*, followed by 11 mm against *Bacillus subtilis* and 10 mm against *Candida albicans*. When compared to the positive control (Kanamycin), these results validate the potent antimicrobial activity of the synthesized AgNPs. Collectively, these findings underscore that the green synthesis techniques of AgNPs using plant extracts are seen as a promising option that aids the elimination of hazardous reducing agents. However, this study lacks the compound-specific extraction and the optimization of environmental conditions for better synthesis of AgNPs. Future research could focus on the isolation of key phytochemicals involved in AgNPs synthesis as well as optimization of environmental parameters to narrow the particle size distribution and enhance long-term stability.

Acknowledgements: Authors are grateful to the Department of Chemistry, Amrit Campus, Tribhuvan University, Nepal for laboratory facilities.

Conflict of interest: The authors declare they have no competing interests.

References

1. Hamedi S, Shojaosadati SA. Rapid and green synthesis of silver nanoparticles using Diospyros lotus extract: Evaluation of their biological and catalytic activities. Polyhedron. 2019; 171: 172–180. doi: 10.1016/j.poly.2019.07.010.
2. Selvan DA, Mahendiran D, Kumar RS, Rahiman AK, Selvan DA. Garlic, green tea and turmeric extracts-mediated green synthesis of silver nanoparticles: Phytochemical, antioxidant and in vitro cytotoxicity studies. Journal of photochemistry and photobiology b: Biology. 2018; 180: 243–252. doi: 10.1016/j.jphotobiol.2018.02.014.
3. Thiruvengadam M, Chung IM, Gomathi T; et al. Synthesis, characterization and pharmacological potential of green synthesized copper nanoparticles. Bioprocess and biosystems engineering. 2019; 42: 1769–1777. doi: 10.1007/s00449-019-02173-y.
4. Sharma AK, Rana K, Shrestha S; et al. A comparative Study on Synthesis, Characterization and Antibacterial Activity of Green vis-a-vis Chemically Synthesized Silver Nanoparticles. Amrit Research Journal. 2022; 3(01): 75–83. doi: 10.3126/arj.v3i01.50499.
5. Abdel-Raouf N, Al-Enazi NM, Ibraheem IBM. Green biosynthesis of gold nanoparticles using Galaxaura elongata and characterization of their antibacterial activity. Arabian Journal of Chemistry. 2017; 10: S3029–S3039. doi: 10.1016/j.arabjc.2013.11.044.
6. Zia R, Riaz M, Farooq N; et al. Antibacterial activity of Ag and Cu nanoparticles synthesized by chemical reduction method: A comparative analysis. Materials Research Express. 2018; 5(7): 075012. doi: 10.1088/2053-1591/aacf70.

7. Yadi M, Mostafavi E, Saleh B; et al. Current developments in green synthesis of metallic nanoparticles using plant extracts: A review. Artificial Cells, Nanomedicine, and Biotechnology. 2018; 46(Suppl. 3): 336–343. doi: 10.1080/21691401.2018.1492931.
8. Abou El-Nour KMM, Eftaiha A, Al-Warthan A; et al. Synthesis and applications of silver nanoparticles. Arabian Journal of Chemistry. 2010; 3(3): 135–140. doi: 10.1016/j.arabjc.2010.04.008.
9. Manosalva N, Tortella G, Cristina Diez M; et al. Green synthesis of silver nanoparticles: Effect of synthesis reaction parameters on antimicrobial activity. World Journal of Microbiology and Biotechnology. 2019; 35: 1–9. doi: 10.1007/s11274-019-2664-3.
10. Sajid M, Płotka-Wasylka J. Nanoparticles: Synthesis, characteristics, and applications in analytical and other sciences. Microchemical Journal. 2020; 154: 104623. doi: 10.1016/j.microc.2020.104623.
11. Dehghanizade S, Arasteh J, Mirzaie A. Green synthesis of silver nanoparticles using Anthemis atropatana extract: Characterization and in vitro biological activities. Artificial Cells, Nanomedicine, and Biotechnology. 2017; 46(1): 160–168. doi: 10.1080/21691401.2017.1304402.
12. Mousavi B, Tafvizi F, Zaker Bostanabad S. Green synthesis of silver nanoparticles using Artemisia turcomanica leaf extract and the study of anti-cancer effect and apoptosis induction on gastric cancer cell line (AGS). Artificial Cells, Nanomedicine, and Biotechnology. 2018; 46(suppl. 1): 499–510. doi: 10.1080/21691401.2018.1430697.
13. Alkhulaifi MM, Alshehri JH, Alwehaibi MA; et al. Green synthesis of silver nanoparticles using Citrus limon peels and evaluation of their antibacterial and cytotoxic properties. Saudi Journal of Biological Sciences. 2020; 27(12): 3434–3441. doi: 10.1016/j.sjbs.2020.09.031.
14. Abbasi N, Ghaneialvar H, Moradi R; et al. Formulation and characterization of a novel cutaneous wound healing ointment by silver nanoparticles containing Citrus lemon leaf: A chemobiological study. Arabian Journal of Chemistry. 2021; 14(7): 103246. doi: 10.1016/j.arabjc.2021.103246.
15. Bedlovičová Z, Strapáč I, Baláž M; et al. A brief overview on antioxidant activity determination of silver nanoparticles. Molecules. 2020; 25(14): 3191. doi: 10.3390/molecules25143191.
16. Jini D, Sharmila S. Green synthesis of silver nanoparticles from Allium cepa and its in vitro antidiabetic activity. Materials Today: Proceedings. 2020; 22: 432–438. doi: 10.1016/j.matpr.2019.07.672.
17. Kumar V, Singh S, Srivastava B; et al. Green synthesis of silver nanoparticles using leaf extract of Holoptelea integrifolia and preliminary investigation of its antioxidant, anti-inflammatory, antidiabetic and antibacterial activities. Journal of Environmental Chemical Engineering. 2019; 7(3): 103094. doi: 10.1016/j.jece.2019.103094.
18. Tan P, Li H S, Wang J; et al. Silver nanoparticle in biosensor and bioimaging: Clinical perspectives. Biotechnology and Applied Biochemistry. 2021; 68(6): 1236–1242.
19. Zhang X F, Liu Z G, Shen W; et al. Silver nanoparticles: Synthesis, characterization, properties, applications, and therapeutic approaches. International journal of molecular sciences. 2016; 17(9): 1534. doi: 10.3390/ijms17091534.
20. Zheng K, Setyawati MI, Leong D T; et al. Antimicrobial silver nanomaterials. Coordination Chemistry Reviews. 2018; 357: 1–17. doi: 10.1016/j.ccr.2017.11.019.
21. Moodley JS, Krishna SBN, Pillay K; et al. Green synthesis of silver nanoparticles from Moringa oleifera leaf extracts and its antimicrobial potential. Advances in Natural Sciences: Nanoscience and Nanotechnology. 2018; 9(1): 015011. doi: 10.1088/2043-6254/aaabb2.
22. Salem SS, Fouda A. Green synthesis of metallic nanoparticles and their prospective biotechnological applications: An overview. Biological trace element research. 2021; 199(1): 344–370. doi: 10.1007/s12011-020-02138-3.
23. Vijayaraghavan K, Ashokkumar T. Plant-mediated biosynthesis of metallic nanoparticles: A review of literature, factors affecting synthesis, characterization techniques and applications. Journal of environmental chemical engineering. 2017; 5(5): 4866–4883. doi: 10.1016/j.jece.2017.09.026.
24. Ali S G, Jalal M, Ahmad H; et al. Green Synthesis of Silver Nanoparticles from Camellia sinensis and Its Antimicrobial and Antibiofilm Effect against Clinical Isolates. Materials. 2022; 15(19): 6978. doi: 10.3390/ma15196978.
25. Khac KT, Phu HH, Thi HT; et al. Biosynthesis of silver nanoparticles using tea leaf extract (camellia sinensis) for photocatalyst and antibacterial effect. Heliyon. 2023; 9(10). doi: 10.1016/j.heliyon.2023.e20707.
26. Demir A. Green-synthesized silver nanoparticles from Camellia sinensis: Mechanistic insights into phenolic-mediated multifunctional biological activities. BMC Plant Biology. 2025; 25(1). doi: 10.1186/s12870-025-07881-0.

27. Wirwis A, Sadowski Z. Green Synthesis of Silver Nanoparticles: Optimizing Green Tea Leaf Extraction for Enhanced Physicochemical Properties. ACS Omega. 2023; 8(33): 30532–30549. doi: 10.1021/acsomega.3c03775.
28. Xia EH, Li FD, Tong W; et al. Tea plant information archive: A comprehensive genomics and bioinformatics platform for tea plant. Plant biotechnology journal. 2019; 17(10): 1938–1953. doi: 10.1111/pbi.13111.
29. Fang Y, Hong CQ, Chen FR; et al. Green synthesis of nano silver by tea extract with high antimicrobial activity. Inorganic Chemistry Communications. 2021; 132: 108808. doi: 10.1016/j.inoche.2021.108808.
30. Loo YY, Chieng BW, Nishibuchi M; et al. Synthesis of silver nanoparticles by using tea leaf extract from Camellia Sinensis. International Journal of Nanomedicine. 2012; 7: 4263–4267. doi: 10.2147/IJN.S33344.
31. Jain S, Mehata MS. Medicinal Plant Leaf Extract and Pure Flavonoid Mediated Green Synthesis of Silver Nanoparticles and their Enhanced Antibacterial Property. Scientific Reports. 2017; 7(1). doi: 10.1038/s41598-017-15724-8.
32. Malapermal V, Botha I, Krishna SBN; et al. Enhancing antidiabetic and antimicrobial performance of Ocimum basilicum, and Ocimum sanctum (L.) using silver nanoparticles. Saudi Journal of Biological Sciences. 2017; 24(6): 1294–1305. doi: 10.1016/j.sjbs.2015.06.026.
33. Parthiban E, Manivannan N, Ramanibai R; et al. Green synthesis of silver-nanoparticles from Annona reticulata leaves aqueous extract and its mosquito larvicidal and anti-microbial activity on human pathogens. Biotechnology reports. 2019; 21: e00297. doi: 10.1016/j.btre.2018.e00297.
34. Shaik MR, Khan M, Kuniyil M; et al. Plant-extract-assisted green synthesis of silver nanoparticles using Origanum vulgare L. extract and their microbicidal activities. Sustainability. 2018; 10(4): 913. doi: 10.3390/su10040913.
35. Sana SS, Dogiparthi LK. Green synthesis of silver nanoparticles using Givotia moluccana leaf extract and evaluation of their antimicrobial activity. Materials Letters. 2018; 226: 47–51. doi: 10.1016/j.matlet.2018.05.009.
36. Parajuli S, Nepal P, Awasthi GP; et al. Synthesis, characterization and antimicrobial study of silver nanoparticles using methanolic fraction of Artemisia vulgaris leaf. Bibechana. 2024; 21(1): 63–73. doi: 10.3126/bibechana.v21i1.60018.
37. Mistry H, Thakor R, Patil C; et al. Biogenically proficient synthesis and characterization of silver nanoparticles employing marine procured fungi Aspergillus brunneoviolaceus along with their antibacterial and antioxidative potency. Biotechnology Letters. 2020; 43(1): 307–316. doi: 10.1007/s10529-020-03008-7.
38. Otunola GA, Afolayan AJ. In vitro antibacterial, antioxidant and toxicity profile of silver nanoparticles green-synthesized and characterized from aqueous extract of a spice blend formulation. Biotechnology & Biotechnological Equipment. 2018; 32(3): 724–733. doi: 10.1080/13102818.2018.1448301.
39. Smith B. Infrared Spectral Interpretation, In The Beginning I: The Meaning of Peak Positions, Heights, and Widths. Spectroscopy. 2024; 39: 18–24. doi: 10.56530/spectroscopy.fi6379n1.
40. Rolim WR, Pelegrino MT, de Araújo Lima B; et al. Green tea extract mediated biogenic synthesis of silver nanoparticles: Characterization, cytotoxicity evaluation and antibacterial activity. Applied Surface Science. 2019; 463: 66–74. doi: 10.1016/j.apsusc.2018.08.203.
41. El deeb BA, Faheem GG, Bakhit MS. Biosynthesis of silver nanoparticles by Talaromyces funiculosus for therapeutic applications and safety evaluation. Scientific Reports. 2025; 15(1): 13750. doi: 10.1038/s41598-025-95899-7.
42. Aref MS, Salem SS. Bio-callus synthesis of silver nanoparticles, characterization, and antibacterial activities via Cinnamomum camphora callus culture. Biocatalysis and Agricultural Biotechnology. 2020; 27: 101689. doi: 10.1016/j.bcab.2020.101689.
43. Singh J, Mehta A, Rawat M; et al. Green synthesis of silver nanoparticles using sun dried tulsi leaves and its catalytic application for 4-Nitrophenol reduction. Journal of Environmental Chemical Engineering. 2018; 6(1): 1468–1474. doi: 10.1016/j.jece.2018.01.054.
44. Behravan M, Hossein Panahi A, Naghizadeh A; et al. Facile green synthesis of silver nanoparticles using Berberis vulgaris leaf and root aqueous extract and its antibacterial activity. International Journal of Biological Macromolecules. 2019; 124: 148–154. doi: 10.1016/j.ijbiomac.2018.11.101.
45. Ahamed M, Majeed Khan MA, Siddiqui MKJ; et al. Green synthesis, characterization and evaluation of biocompatibility of silver nanoparticles. Physica E: Low-dimensional Systems and Nanostructures. 2011; 43(6): 1266–1271. doi: 10.1016/j.physe.2011.02.014.
46. Mortazavi-Derazkola S, Ebrahimzadeh MA, Amiri O; et al. Facile green synthesis and characterization of Crataegus microphylla extract-capped silver nanoparticles (CME@Ag-NPs) and its potential antibacterial and anticancer activities

against AGS and MCF-7 human cancer cells. Journal of Alloys and Compounds. 2020; 820: 153186. doi: 10.1016/j.jallcom.2019.153186.

47. Reddy GS, Saritha KV, Reddy YM; et al. Eco-friendly synthesis and evaluation of biological activity of silver nanoparticles from leaf extract of Indigofera barberi Gamble: An endemic plant of Seshachalam Biosphere Reserve. SN Applied Sciences. 2019; 1: 968. doi: 10.1007/s42452-019-1008-0.
48. Hussain Z, Jahangeer M, Sarwar A; et al. Synthesis and characterization of silver nanoparticles mediated by the mentha piperita leaves extract and exploration of its antimicrobial activities. Journal of the Chilean Chemical Society. 2023; 68(2): 5865-5870. doi: 10.4067/s0717-97072023000205865.
49. Ahmad N, Ansari MA, Al-Mahmeed A; et al. Biogenic silver nanomaterials synthesized from Ocimum sanctum leaf extract exhibiting robust antimicrobial and anticancer activities: Exploring the therapeutic potential. Heliyon. 2024; 10(15): e35486. doi: 10.1016/j.heliyon.2024.e35486.
50. Koteswara Rao P, Srinivasulu S, Ravindra nadh M; et al. Anticancer and antibacterial activity of green synthesized silver nanoparticles using Adina cordifolia. Materials Today: Proceedings. 2021; 43: 1700-1706. doi: 10.1016/j.matpr.2020.10.043.
51. Ismail E, Mohamed A, Elzwawy A; et al. Comparative Study of Callistemon citrinus (Bottlebrush) and Punica granatum (Pomegranate) Extracts for Sustainable Synthesis of Silver Nanoparticles and Their Oral Antimicrobial Efficacy. Nanomaterials. 2024; 14(11): 974. doi: 10.3390/nano14110974.
52. Keskın D, Oskay D, Oskay M. Antimicrobial activity of selected plant spices marketed in the West Anatolia. International Journal of Agriculture and Biology. 2010; 12(6): 916-920.
53. Safarpoor M, Ghaedi M, Asfaram A; et al. Ultrasound-assisted extraction of antimicrobial compounds from Thymus daenensis and Silybum marianum: Antimicrobial activity with and without the presence of natural silver nanoparticles. Ultrasonics Sonochemistry. 2018; 42: 76-83. doi: 10.1016/j.ultsonch.2017.11.001.
54. Bruna T, Maldonado-Bravo F, Jara P; et al. Silver Nanoparticles and Their Antibacterial Applications. International Journal of Molecular Sciences. 2021; 22(13): 7202. doi: 10.3390/ijms22137202.
55. Juzer T, Soundharajan R, Srinivasan H. Camellia sinensis mediated silver nanoparticles: Eco-friendly antimicrobial agent to control multidrug resistant Gram-positive Staphylococcus aureus. Discover Nano. 2025; 20(1). doi: 10.1186/s11671-025-04278-8.
56. Tijani NA, Afolabi AO, Mutanule F; et al. Exploring the anticandida potentials of nanoparticles fabricated from tea leaf (Camellia sinensis) extracts: A systematic review. Discover Materials. 2025; 5(1): 14. doi: 10.1007/s43939-025-00196-9.
57. Lee NY, Ko WC, Hsueh PR. Nanoparticles in the Treatment of Infections Caused by Multidrug-Resistant Organisms. Frontiers in Pharmacology. 2019; 10: 10. doi: 10.3389/fphar.2019.01153.
58. Skłodowski K, Chmielewska-Deptuła SJ, Piktel E; et al. Metallic Nanosystems in the Development of Antimicrobial Strategies with High Antimicrobial Activity and High Biocompatibility. International Journal of Molecular Sciences. 2023; 24(3): 2104. doi: 10.3390/ijms24032104.
59. El deeb BA, Faheem GG, Bakhit MS. Antimicrobial Activities of Biogenic Silver Nanoparticles Synthesized by Curvularia spicifera. Sohag Journal of Sciences. 2025; 10(1): 95-102. doi: 10.21608/sjsci.2024.336812.1233.